American Mineralogist, Volume 91, pages 1049–1054, 2006

Sound velocities and elastic constants of $ZnAl_2O_4$ spinel and implications for spinel-elasticity systematics

HANS J. REICHMANN[1,*] AND STEVEN D. JACOBSEN[2,†]

[1]Geoforschungszentrum Potsdam, Section 4.1, Telegrafenberg, 14473 Potsdam, Germany
[2]Geophysical Laboratory, Carnegie Institution of Washington, 5251 Broad Branch Road NW, Washington, D.C. 20015, U.S.A.

ABSTRACT

The pressure dependence of the sound velocities, single-crystal elastic constants, and shear and adiabatic bulk moduli of a natural gahnite ($ZnAl_2O_4$) spinel have been determined to ~9 GPa by gigahertz ultrasonic interferometry in a diamond anvil cell. The elastic constants of gahnite are (in GPa): C_{11} = 290(3), C_{12} = 169(4), and C_{44} = 146(2). The elastic constants C_{11} and C_{12} have similar pressure derivatives of 4.48(10) and 5.0(8), while the pressure derivative of C_{44} is 1.47(3). In contrast to magnetite, gahnite does not exhibit C_{44} mode softening over the experimental pressure range. The adiabatic bulk modulus K_{S0} is 209(5) GPa, with pressure derivative K_S' = 4.8(3), and the shear modulus G_0 = 104(3) GPa, with G' = 0.5(2). Gahnite, along with chromite ($FeCr_2O_4$) and hercynite ($FeAl_2O_4$) are the least compressible of the naturally occurring oxide spinels. Evaluation of Birch's Law for isostructural minerals indicates that spinels containing transition metals on both the $^{[4]}A$ and $^{[6]}B$ sites follow a trend about five times more negative than oxide and silicate-spinel phases without any, or only one transition metal.

Keywords: Spinel, sound wave velocities, elastic properties, Birch's Law

INTRODUCTION

Minerals with the spinel structure and general formula AB_2O_4 are among the most common non-silicate oxides in the Earth's crust and upper mantle. Spinels have cubic symmetry (space group $Fd3m$, 8 formula units per unit cell), and have an essentially cubic close-packed array of oxygen. A characteristic feature of this structure is the ability to host a wide range of divalent, trivalent, and tetravalent cations; over 100 natural and synthetic phases adopt this structure. In the normal spinel structure, the A cations occupy the tetrahedral site and B cations occupy the octahedral site ($^{[4]}A^{[6]}B_2O_4$). Inverse spinels contain four-coordinated B cations, while the six-coordinated site contains a mixture of A and B cations [$^{[4]}B^{[6]}(B,A)_2O_4$]. In addition to magnesioferrite–magnetite ($MgFe_2O_4$–Fe_3O_4) and spinel–hercynite ($MgAl_2O_4$–$FeAl_2O_4$), the zinc-spinels franklinite–gahnite ($ZnFe_2O_4$–$ZnAl_2O_4$) form a limited solid solution at high temperature and are important accessory phases in various rock types, but most notably in the Franklin marble and skarn deposits (Carvalho and Sclar 1988; Frondel and Baum 1974). Moreover, the silicate spinel, ringwoodite γ-$(Mg,Fe)_2SiO_4$, is expected to be the dominant phase in the lower part of Earth's transition zone between about 520 and 660 km depth. Because spinels exhibit pressure-induced phase changes (Fei et al. 1999; Funamori et al. 1998; Irifune et al. 2002; Levy et al. 2000), they are often used as model minerals for deep-Earth mineralogy. The spinel structure type is also of practical importance to industrial applications; the ferrites are composed of Fe_2O_3 mixed with various Mn, Zn, Ni, and Mg oxides and are strong magnets utilized in many electronic, communications, and power-switching devices.

Most previous studies of spinel elasticity have relied on static compression (X-ray diffraction) to determine the isothermal bulk modulus K_{T0} and $K_T' = dK_T/dP$ from pressure-volume data (Chang and Barsch 1973; Haavik et al. 2000; Hazen 1993; Irifune et al. 2002; Levy et al. 2000, 2001; Mao et al. 1974; Yutani et al. 1997). Pressure dependence of the single-crystal elastic constants (C_{ij}) for natural spinels have only been reported for spinel (Yoneda 1990) and magnetite (Reichmann and Jacobsen 2004), thus, single-crystal elasticity systematics are only now emerging. Due to the relative structural simplicity of close-packed spinels, single-crystal elasticity data will provide a better understanding of the different effects of pressure on structure and bonding because they can be modeled to a first approximation as ionic compounds with bond strengths according to Coulombic forces (e.g., Hazen 1993). However, simple theory is not always effective when close-packed structures contain transition metals as nearest-neighbors.

It was shown recently (Reichmann and Jacobsen 2004) by means of gigahertz-interferometry measurements on the inverse spinel magnetite [$Fe^{3+}(Fe^{2+}Fe^{3+})O_4$] that the 3$d$ transition-metal element Fe has a dramatic effect on the elastic high-pressure behavior, especially on C_{44}. This modulus has a negative pressure derivative and was interpreted to be a soft mode preceding the structure transition at ~20 GPa (Reichmann and Jacobsen 2004). It is now of special interest to investigate how the single crystal and bulk elastic properties

* E-mail: Hanni@gfz-potsdam.de
† Present Address: Department of Geological Sciences, Northwestern University, Evanston, IL 60208, U.S.A.

0003-004X/06/0007–1049$05.00/DOI: 10.2138/am.2006.2122

of spinels are affected by other transition metals (e.g., Zn and Cr). Comparisons can then be made to other spinels without (or having two) transition metals occupying the cation sites.

Levy et al. (2001) determined the compressibility of gahnite and obtained an unusually high $K' = 7.62(9)$ with $K'' = -0.1022$ GPa^{-1} (implied value) and $K_0 = 201.7(9)$ GPa. Because the authors were able to reach very high pressures (~43 GPa), the high-precision X-ray data were sufficient to refine K'. In this paper we report the pressure dependence of the full set of the single-crystal elastic constants (C_{ij}) and the aggregate moduli (G and K_S) of gahnite spinel. The GHz-ultrasonic measurements were performed using a natural sample under hydrostatic compression in diamond anvil cell to a maximum pressure of 8.6 GPa. Finally, we compile current spinel elasticity data and recognize two distinct sound velocity trends for spinels without any, or only one transition metal, and spinels containing two transition metals.

Experimental methods

Sample characterization

The natural gahnite sample is from Stratford, Alleghan, North Carolina. It showed an octahedral form making it possible to identify and to cut sections parallel to the (100) and (111) planes to within a few degrees. Microprobe analysis gives a bulk chemical composition of $(Zn_{0.74}Fe_{0.18}Mg_{0.08})Al_{1.99}O_4$. The lattice constant a = 8.0985(2) Å was determined by the eight-position centering of 15 reflections on the Huber diffractometer at Bayerisches Geoinstitut, and is in good agreement with the synthetic crystal studied by Levy et al. (2001) with a = 8.09117(5) Å obtained by powder X-ray diffraction. The calculated density of our sample is 4464 (kg/m^3).

High-pressure ultrasonic interferometry

The polished gahnite samples used for GHz-interferometry in a diamond anvil cell had a diameter of about 120 µm and a thickness of 45 µm Special effort was made to ensure parallelism of the polished planes, which is a prerequisite to obtain usable interference patterns.

Sound wave velocities of gahnite were determined at ambient and elevated pressure in a diamond anvil cell using GHz-interferometry (Reichmann et al. 1998; Spetzler et al. 1993). We recently added shear-wave capabilities to the GHz-technique, allowing determination of full sets of elastic constants for minerals at ambient (Jacobsen et al. 2004a) and high pressures (Reichmann and Jacobsen 2004). A detailed description of the new method is given by (Jacobsen et al. 2005). Briefly, a tone burst generated from a ZnO thin-film piezo-transducer with carrier frequencies between 0.5–2 GHz and 20–100 ns in duration are introduced into the sample through the diamond by mechanical contact. Strain waves reflected at the near and far facets of the parallel-plate sample overlap in time when the input tone burst is longer than the travel-time through the sample. This superposition gives rise to an interference pattern when the frequency (f) is scanned, from which the round-trip travel time (t) of the sound waves through the sample is determined from Δf of adjacent extrema. Given the sample length (l), longitudinal and transverse velocities ($V_{P,S}$) are obtained by:

$$V_{P,S} = 2l/t_{P,S} \quad (1)$$

Figure 1a shows a raw interference pattern for shear waves in gahnite at 8.0 GPa, from which a travel time t_S = 16.06(2) ns was obtained (Fig. 1b). We note that although the absolute uncertainty in C_{ij} at ambient pressure is dominated by the uncertainty in the length, uncertainties in the variation of C_{ij} with pressure (the derivatives) are very small because the relative travel-time uncertainties are on the order of a few parts in 10^3.

Hydrostatic conditions in the sample chamber of the DAC were achieved by using a 16:3:1 methanol-ethanol-water mixture. To avoid the flow of fluid between the sample and the diamond, a small amount of silica aerogel was added to the liquid pressure medium (Reichmann and Jacobsen 2004). The pressure was determined before and after each run using ruby fluorescence (Mao et al. 1986).

Sample length determination at high pressure

Sample thickness variation with pressure in the cubic system was determined by the relation:

$$(l/l_0) = (V/V_0)^{1/3} \quad (2)$$

where V is volume and V_0 is the initial volume. V/V_0 was calculated using the third-order Birch-Murnaghan equation of state (BM3 EoS) parameters K_{T0} = 201.7 (GPa) and K' = 7.62 (K'' = –0.1022 GPa^{-1} implied) from the compression study of Levy et al. (2001). Although the value of K' from Levy et al. (2001) seems high compared to the often assumed value of 4.0, we tested the effects of varying K' on the calculated sample length and found below 10 GPa the choice had no significant influence on the sample length, and hence the calculated elastic constants. In Table 1, the calculated sample length is reported using both values of K', and we note that at the highest experimental pressure (8.6 GPa), the difference between the sample length calculated with K' = 4 and K' = 7.62 is only 0.06%.

Results

Cubic crystals have three independent elastic constants: C_{11}, C_{12}, and C_{44} (e.g., Nye 1985). To obtain the full set of C_{ij} it is necessary to obtain the sound velocities in various crystallographic directions. The elastic constants of gahnite were calculated from the following three pure-mode solutions of the Christoffel equations (in Brugger 1965):

$$\rho\,(V_P^{[100]})^2 = C_{11} \quad (3)$$

$$\rho\,(V_S^{[100]})^2 = C_{44} \quad (4)$$

$$\rho\,(V_P^{[111]})^2 = (C_{11} + 4C_{44} + 2C_{12})/3 \quad (5)$$

where ρ is the density and $V_{P,S}$ are sound velocities in the superscript [uvw] propagation direction.

Ambient pressure experiments were performed using "thick" samples measuring 248 µm in length with a nominal accuracy of ±1 µm, resulting in absolute uncertainties in C_{ij} of about one in 100 GPa. Diamond-cell samples measuring ~45 µm thick were prepared, and their initial lengths were calculated using their measured P_0 travel times and the "thick sample" velocities. Initial sample lengths were 46.9(2) and 45.6(2) µm for the $V_P^{[100]}$ samples, 46.9(2) µm for the $V_P^{[111]}$ sample, and 47.4(2) µm for the $V_S^{[100]}$ sample. Variation of sample length with pressure for two different equations of state is listed in Table 1.

Sound velocities in gahnite in various crystallographic directions and at various pressures are listed in Table 2. The calculated elastic modulus C_{ij} of gahnite are: C_{11} = 290(3) GPa, C_{12} = 169(4)

Table 1. Calculated sample length at high pressure*

P (GPa)	Sample length (µm)†	Sample length (µm) ‡
0	46.9	46.9
1.73	46.77	46.77
2.46	46.71	46.72
2.98	46.68	46.68
3.45	46.64	46.65
4.32	46.58	46.59
5.44	46.50	46.52
8.60	46.29	46.32

* Ruby fluorescence pressures with nominal precision of 0.05 GPa.
† Calculated using K_{T0} = 201.7 GPa with K' = 4.
‡ Calculated using K_{T0} = 201.7 GPa with K' = 7.62, K'' = –0.1022 GPa^{-1} (Levy et al. 2001).

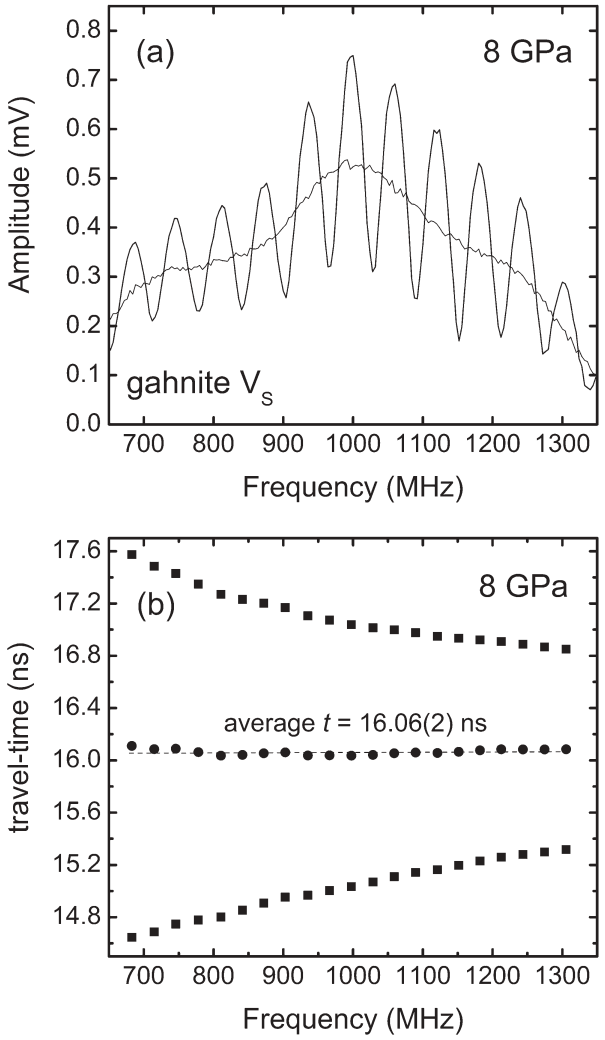

FIGURE 1. (**a**) GHz-ultrasonic interference pattern for shear waves in gahnite at 8 GPa. (**b**) Travel times calculated from this spectrum for the correct (filled circles) and nearest fringes (filled squares) in the fit of integer solutions to the number of wavelengths in the sample.

GPa, and C_{44} = 146(2) GPa, with the pressure derivatives $dC_{11}/dP = C'_{11}$= 4.48(10), $dC_{12}/dP = C'_{12}$= 5.0(8), and $dC_{44}/dP = C'_{44}$ = 1.47(3). The adiabatic bulk modulus is K_{S0} = 209(5) GPa, the shear modulus G_0 = 104(3) GPa (average of Hashin Shtrikman bounds), dK_S/dP = 4.8(3) and dG/dP = 0.5(2). The uncertainty of K_{S0} and G is due to the uncertainties of travel-time and sample length determinations whereas the uncertainty of the pressure derivatives is calculated from linear fits. The calculated data of the longitudinal and shear velocities are fitted to a linear curve.

$$V_P = 8832(60) + 47.6(4)\ P \text{ (m/s)} \quad (6)$$

$$V_S = 4824(50) + 0.7(6)\ P \text{ (m/s)} \quad (7)$$

DISCUSSION

The three independent elastic constants of gahnite are shown as a function of pressure in Figure 2. The pressure derivatives

TABLE 2. Sound velocities of $ZnAl_2O_4$ gahnite at various pressures*

P (GPa)	$v_P^{[100]}$† (m/s)	P (GPa)	$v_P^{[111]}$† (m/s)	P (GPa)	$v_S^{[100]}$† (m/s)
0	8058(35)	0	9509(30)	0	5720(20)
3.28	8193(28)	1.73	9614(29)	5.10	5812(14)
5.34	8285(36)	2.46	9633(39)	5.50	5816(10)
6.39	8326(40)	2.98	9695(40)	5.80	5816(14)
1.21	8096(21)	3.45	9708(40)	6.30	5831((13)
2.18	8148(21)	4.32	9720(50)	6.70	5831(12)
2.94	8175(22)	5.44	9824(70)	7.00	5836(9)
3.42	8191(22)			7.30	5835(10)
3.88	8214(29)			7.60	5845(10)
4.41	8237(29)			8.00	5847(9)
5.46	8277(37)			8.30	5864(12)
5.56	8283(37)			8.60	5867(13)

* Ruby fluorescence pressures with nominal precision of 0.05 GPa.
† Superscript [*uvw*] gives the direction of elastic wave propagation.

C'_{11} and C'_{12} of gahnite are very similar to each other, while C'_{44} is considerably lower. It is interesting to note that this is also true for spinel $MgAl_2O_4$ (Yoneda 1990) and magnetite Fe_3O_4 (Reichmann and Jacobsen 2004) (Table 3). It seems that it is a general feature of the spinel structure that $C'_{11} \cong C'_{12}$ and $C'_{44} << C'_{11}$.

Table 3 summarizes the elastic moduli and their pressure derivatives of various spinels. Whereas Yoneda (1990) reported first and second derivatives of the elastic constants and bulk modulus from polynomial fits to the data, in the present work the C_{ij} and moduli are linear within error so only first derivatives are reported. Based on a comparison of gahnite with spinel, Mg-Zn substitution on the tetrahedral site appears to reduce the pressure dependence of C_{11} and C_{12}, whereas C'_{44} is identical within error. The sign of dC_{44}/dP is positive (Table 3), in contrast with both magnetite (Reichmann and Jacobsen 2004) and iron-rich magnesiowüstite (Jacobsen et al. 2005), which exhibit negative C_{44} derivatives. If C_{44} mode softening in spinels is associated with pressure-induced phase transitions, one might conclude that $ZnAl_2O_4$ should undergo a possible phase transition at a much higher pressure than Fe_3O_4. This is in agreement with the work of Levy et al. (2001) who performed X-ray diffraction experiments to 43 GPa without detecting a phase transformation, whereas magnetite exhibits a phase transition at $P > 20$ GPa (Fei et al. 1999; Haavik et al. 2000; Mao et al. 1974; Pasternak et al. 1994).

The adiabatic bulk modulus of gahnite, K_{S0} = 209(5), is about 5% higher than for $MgAl_2O_4$ spinel, and about 12% higher than that of magnetite. The isothermal bulk modulus K_{T0} of gahnite, determined by powder X-ray diffraction (Levy et al. 2001) is 201.7(9) GPa, which is only 3.5% lower than the reported value of K_{S0} here. However, the shear modulus of gahnite is 7% lower than G_0 of $MgAl_2O_4$ spinel, but is about 70% higher than the shear modulus of magnetite Fe_3O_4, indicating that Zn does not have the same drastic effect of Fe in reducing C_{44}.

The pressure dependences of the aggregate bulk and shear moduli (K_S and G, respectively) of gahnite, magnetite (Reichmann and Jacobsen 2004), $MgAl_2O_4$ spinel (Yoneda 1990) as well as the isothermal bulk modulus of synthetic gahnite (Levy et al. 2001) are plotted in Figure 3. The pressure derivatives of the adiabatic bulk moduli K_S of gahnite and magnetite (Reichmann and Jacobsen 2004), are very similar with K'_S = 4.8(3) and 5.1(1), respectively. The pressure derivative K'_T = 7.62(9) for gahnite reported by Levy et al. (2001) is measurably higher but it is not clear if this difference is intrinsic or due to experimental

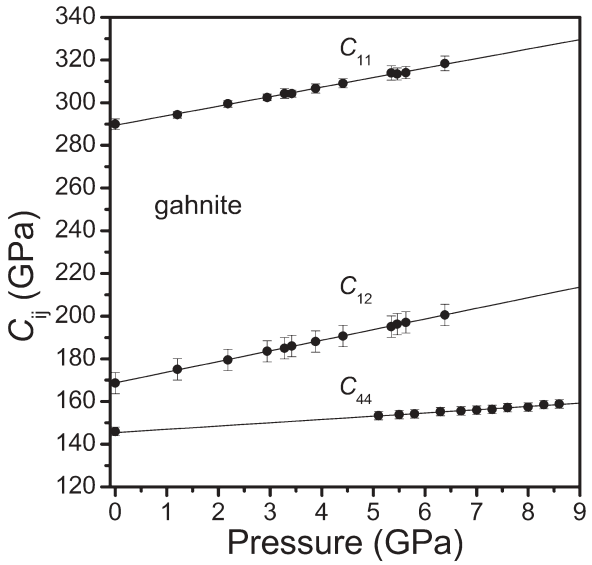

FIGURE 2. Variation of the single-crystal elastic constants (C_{11}, C_{12}, and C_{44}) of gahnite with pressure. Solid lines are linear fits to the data.

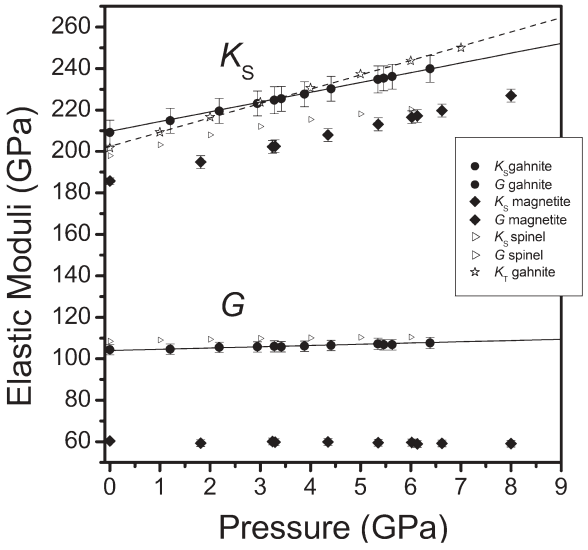

FIGURE 3. Aggregate bulk and shear moduli of gahnite at high pressure from the current study (filled circles). Also shown are K_S and G for magnetite (filled diamonds; Reichmann and Jacobsen 2004) and $MgAl_2O_4$ spinel (open triangles; Yoneda 1990). Calculated isothermal bulk modulus (K_T) of gahnite is shown by open stars (Levy et al. 2001). The solid line is a linear fit to the GHz-ultrasonic gahnite data. The dashed line is a second-order polynomial fit to the static X-ray data for gahnite (Levy et al. 2001).

factors. Pressure derivatives of the shear modulus for gahnite $G' = 0.5(2)$ and $MgAl_2O_4$ $G' = 0.61$ (Yoneda 1990) are both positive and similar in contrast with magnetite, which has a slightly negative or invariant $G' = -0.1(1)$ (Reichmann and Jacobsen 2004). Low values of G' (< 1) appear to be a common feature of oxide spinels (Table 3) as opposed to magnesium-silicate spinels (G' = 1.3–1.5; Li 2003; Sinogeikin et al. 2003).

Spinel elasticity systematics and Birch's Law

Birch (1961a, 1961b) proposed that at constant mean atomic mass (M), an increase in density would lead to a linearly proportional increase in bulk sound velocity (V_ϕ). Birch's Law is often written:

$$V_\phi = a + b\rho \tag{8}$$

where b is positive. Alternatively, isostructural compounds with varying M plot roughly perpendicular to the iso-M lines, i.e., the velocity vs. density curve of isostructural minerals exhibits a negative slope. In Figure 4 the bulk sound velocity $V_\phi = (V_P^2 - {}^4/_3 V_S^2)^{1/2} = (K_0/\rho)^{1/2}$ is plotted against density for various minerals of the spinel group. As expected, the diagram shows that spinels with only one transition metal at the cation sites exhibit decreasing bulk sound velocities with increasing density. The data for these compounds define roughly a linear curve as proposed by Birch (1961a, 1961b). However, those high density spinels with transition metals at both the [4]A and [6]B sites, i.e., chromite, magnetite, franklinite, and zincochromite, follow a different trend that is about five times more negative (Fig. 4). One conclusion that can be drawn from Figure 4 is that the linearly decreasing V_ϕ with increasing ρ changes slope when two 3d-transition elements occupy both the tetrahedral and octahedral cation sites. The change in slope may indicate that the dominant Coulombic bonding forces assumed for ideal ionic compounds

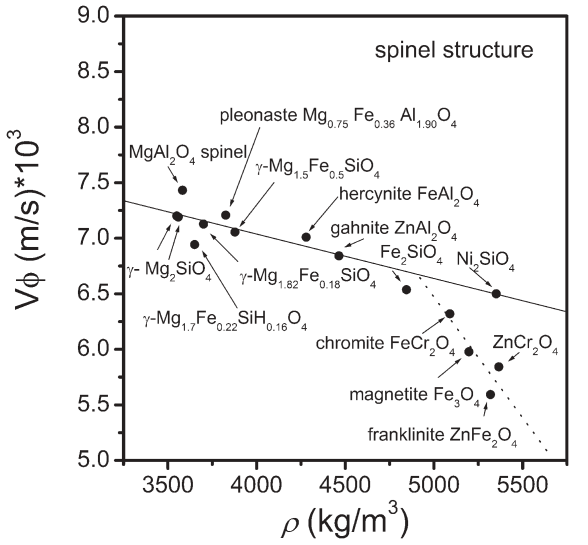

FIGURE 4. Birch's Law revisited; bulk sound velocity $V_\phi = (K_0/\rho)^{1/2}$ as a function of density. Spinel minerals containing transition metals on both [4]A and [6]B sites follow a steeper trend than those without or only one transition metal. Dotted line is a linear fit to only the data points of chromite, magnetite, franklinite, and zincochromite. Solid line is a linear fit to the remaining spinels. γ-Mg_2SiO_4 = Weidner et al. 1984; Hazen 1993; $MgAl_2O_4$ spinel = Yoneda 1990; $FeFe_2O_4$ magnetite = Reichmann and Jacobsen 2004; gahnite = this study; $ZnCr_2O_4$ zincochromite = Levy et al. 2005; Fe_2SiO_4 = Hazen 1993; Ni_2SiO_4 = Bass et al. 1984; $FeCr_2O_4$ chromite = Hearmon 1984; γ-$Mg_{1.7}Fe_{0.22}H_{0.16}SiO_4$ = Jacobsen et al. 2004b; $ZnFe_2O_4$ franklinite = Levy et al. 2000; γ-$Mg_{1.82}Fe_{0.18}SiO_4$ = Sinogeikin and Bass 2001; γ-$Mg_{1.5}Fe_{0.5}SiO_4$ = Sinogeikin et al. 1997; $FeAl_2O_4$ hercynite = Wang and Simmons 1972; $Mg_{0.75}Fe_{0.36}Al_{1.90}O_4$ Pleonaste = Wang and Simmons 1972.

TABLE 3. Compilation of elastic properties of spinel-structured minerals in order of increasing density

Formula (mineral)	Reference	Method and maximum P	ρ_0 (kg/m³)	C_{11} (GPa) C_{11}' C_{11}'' (GPa^{-1})	C_{12} (GPa) C_{12}' C_{12}'' (GPa^{-1})	C_{44} (GPa) C_{44}' C_{44}'' (GPa^{-1})	K (GPa) K' K'' (GPa^{-1})	G (GPa) G'	V_P (m/s) dV_P/dP (ms^{-1}/GPa)	V_S (m/s) dV_S/dP (ms^{-1}/GPa)
$MgAl_2O_4$ (spinel)	Yoneda (1990)	MHz-ultrasonics (P_{max} = 6 GPa)	3578	282.9 5.59 –0.65	155.4 5.69 –0.64	154.8 1.44 –0.19	197.9 5.66 –0.65	110.0 0.61		
γ-$(Mg_{0.91}Fe_{0.09})_2SiO_4$ (ringwoodite)	Sinogeikin et al. (2003)	Brillouin (P_{max} = 16 GPa)	3701	329(2) 6.2(2)	118(3) 2.8(3)	130(2) 0.8(2)	188(3) 4.1(3)	120(2) 1.3(2)	9690(20)	5680(10)
$FeAl_2O_4$ (hercynite)	Wang and Simmons (1972)	MHz-ultrasonics P = 0 GPa	4280	266.0	182.5	133.5	210.3	84.5	8701	4463
$(Zn_{0.74}Fe_{0.18}Mg_{0.08})Al_{1.99}O_4$ (gahnite)	This Study	GHz-ultrasonics (P_{max} = 9 GPa)	4464	290(3) 4.48(10)	169(4) 5.0(8)	146(2) 1.47(3)	209(5) 4.8(3)	104(3) 0.5(2)	8832(60) 47.6(4)	4824(50) 0.7(6)
$ZnAl_2O_4$ (gahnite)	Levy et. (2001)	X-ray (P_{max} = 43 GPa)	4597				201.7(9) 7.62(9)			
γ-Fe_2SiO_4	Hazen (1993)	X-ray (P_{max} = 5 GPa)	4845				207(3) 4.8 (fixed)	104.9		
$FeCr_2O_4$ (chromite)	(Hearmon 1984)		5090				203.3			
$FeFe_2O_4$ (magnetite)	Reichmann and Jacobsen (2004)	GHz-ultrasonics (P_{max} = 9 GPa)	5196	260.5(1.0) 5.14(13)	148.3(3.0) 5.39(10)	63.3(1.5) -0.13(4)	185.7(3.0) 5.1(1)	60.3(3.0) –0.1(1)	7157(30) 47.4(4)	3407(20) –12.5(3)
$ZnFe_2O_4$ (franklinite)	Levy et al. (2000)	X-ray (P_{max} = 37 GPa)	5319				166(3) 9.3(6)			
γ-Ni_2SiO_4	Hazen (1993)	X-ray (P_{max} = 5 GPa)	5339				233(2) 4.8 (fixed)			
$ZnCr_2O_4$ zincochromite	Levy et al. (2005)	X-ray (P_{max} = 21 GPa)	5366				183(4) 7.9(6)			

decreases and the covalent part of the bonding forces becomes mores important. When interatomic forces are parallel to the relative position between atom pairs, the elastic constants satisfy an identity known as the Cauchy condition:

$$\tfrac{1}{2}\,(C_{12} - C_{44}) = P \qquad (9)$$

where P is pressure. At ambient pressure, $\frac{1}{2}(C_{12} - C_{44}) = 0.3$ GPa for $MgAl_2O_4$ spinel (Yoneda 1990) and the Cauchy condition is satisfied within the uncertainty of the C_{ij} (Table 3). As transition metals are added, deviation from the Cauchy identity increases from about 11.4 GPa for gahnite with one transition metal at $^{[4]}$A (this study) to 42.5 GPa for magnetite with transition metals on both $^{[4]}A$ and $^{[6]}B$ (Reichmann and Jacobsen 2004).

The elasticity systematics suggest that the bulk sound velocity of spinels with nearest-neighbor transition metals would be dramatically overestimated by considering Birch's Law for spinels without, or with only one transition metal. As noted above, the V_ϕ vs. ρ curve for transition-metal spinels is about a five times more negative than that for spinels having only one transition metal. Similar changes may be expected for other close-packed oxide structures such as the AO-monoxides and ABO_3-perovskites. The separate Birch trend for transition metal spinels underlines the dramatic affect of transition metal elements on the elastic properties of minerals and the challenge for simple theory to predict their behavior.

ACKNOWLEDGMENTS

We thank T.B. Ballaran for diffractometer time in Bayreuth, C. Schmidt for the sample, and D. Gatta, A. Pavese, and an anonymous referee for their constructive reviews. Jacobsen acknowledges support from the U.S. National Science Foundation EAR-0440112 (Geophysics Program), the Carnegie/DOE Alliance Center (CDAC), the Carnegie Institution of Washington, and the Bayerisches Geoinstitut Visitors Program.

REFERENCES CITED

Bass, J.D., Weidner, D.J., Hamaya, N., Ozima, M., and Akimoto, S. (1984) Elasticity of the olivine and spinel polymorphs of Ni_2SiO_4. Physics and Chemistry of Minerals, 10, 261–272.

Birch, F. (1961a) Composition of the Earth's mantle. Geophysical Journal, 4, 295–311.

——— (1961b) The velocity of compressional waves in rocks to 10 kilobars. Journal of Geophysical Research, 66, 2199–2224.

Brugger, K. (1965) Pure modes for elastic waves in crystals. Journal of Applied Physics, 36, 759–768.

Carvalho, A.V. and Sclar, C.B. (1988) Experimental determination of the $ZnFe_2O_4$-$ZnAl_2O_4$ miscibility gap with application to franklinite-gahnite exsolution intergrowths from the Sterling Hill zinc deposit, New Jersey. Economic Geology and the Bulletin of the Society of Economic Geologists, 83, 1447–1452.

Chang, Z.P. and Barsch, G.R. (1973) Pressure dependence of single crystal elastic constants and anharmonic properties of spinel. Journal of Geophysical Research, 78, 2418–2433.

Fei, Y., Frost, D.J., Mao, H.-K., Prewitt, C.T., and Häusermann, D. (1999) In situ structure determination of the high-pressure phase of Fe_3O_4. American Mineralogist, 84, 203–206.

Frondel, C. and Baum, J.L. (1974) Structure and mineralogy of the Franklin zinc-iron-manganese deposit, New Jersey. Economic Geology and the Bulletin of the Society of Economic Geologists, 69, 157–180.

Funamori, N., Jeanloz, R., Nguyen, J.H., Kavner, A., and Caldwell, W.A. (1998) High-pressure transformations in $MgAl_2O_4$. Journal of Geophysical Research, 103(B9), 20813–20818.

Haavik, C., Stolen, S., Fjelllag, H., Hanfland, M., and Häusermann, D. (2000) Equation of state of magnetite and its high-pressure modification: Thermodynamics of the FeO-system at high pressure. American Mineralogist, 85, 514–523.

Hazen, R.M. (1993) Comparative Compressibilities of Silicate Spinels: Anomalous Behaviour of $(Mg,Fe)_2SiO_4$. Science, 259, 206–209.

Hearmon, R.F.S. (1984) The elastic constants of crystals and other anisotropic materials. In K.H. Hellwege and A.M. Hellwege, Eds., Landolt-Börnstein Tables, III/18, p. 559. Springer Verlag, Berlin.

Irifune, T., Naka, H., Sanehira, T., Inoue, T., and Funakoshi, K. (2002) In situ X-ray observations of phase transitions in $MgAl_2O_4$ spinel to 40 GPa using multianvil apparatus with sintered diamond anvils. Physics and Chemistry of Minerals, 29, 645–654.

Jacobsen, S.D., Spetzler, H.A., Reichmann, H.J., and Smyth, J.R. (2004a) Shear waves in the diamond-anvil cell reveal pressure-induced instability in (Mg,Fe)O. Proceedings of the National Academy of Science, 101(16), 5867–5871.

Jacobsen, S.D., Smyth, J.R., Spetzler, H.A., Holl, C.M., and Frost, D.J. (2004b) Sound velocities and elastic constants of iron-bearing hydrous ringwoodite. Physics of the Earth and Planetary Interiors, 143–144, 47–56.

Jacobsen, S.D., Reichmann, H.J., Kantor, A., and Spetzler, H.A. (2005) A gigahertz-ultrasonic interferometer for the diamond-anvil cell and high-pressure elasticity of some dense iron oxides. In J. Chen, Y. Wang, T.S. Duffy, G. Shen, and L.P. Dobrzhinetskaya, Eds., Advances in High-Pressure Technology for Geophysical Applications, p. 25–48. Elsevier, Amsterdam.

Levy, D., Pavese, A., and Hanfland, M. (2000) Phase transition of synthetic zinc ferrite spinel ($ZnFe_2O_4$) at high pressure, from synchrotron X-ray powder diffraction. Physics and Chemistry of Minerals, 27, 638–644.

Levy, D., Pavese, A., Sani, A., and Pischedda, V. (2001) Structure and compressibility of synthetic $ZnAl_2O_4$ (gahnite) under high-pressure conditions from synchrotron X-ray powder diffraction. Physics and Chemistry of Minerals, 28, 612–618.

Levy, D., Diella, V., Pavese, A., Dapiaggi, M., and Sani, A. (2005) *P-V* equation of State, thermal expansion, and *P-T* stability of synthetic ($ZnCr_2O_4$ spinel). American Mineralogist, 90, 1157–1162.

Li, B. (2003) Compressional and shear wave velocities of ringwoodite γ-Mg_2SiO_4 to 12 GPa. American Mineralogist, 88, 1312–1317.

Mao, H.-K., Takahashi, T., Bassett, W.A., Kinsland, G.L., and Merrill, L. (1974) Isothermal compression of magnetite to 320 Kbar and pressure-induced phase transition. Journal of Geophysical Research, 91, 1165–1170.

Mao, H.-K., Xu, J., and Bell., P.M. (1986) Calibration of the ruby pressure gauge to 800 Kbar under quasi hydrostatic conditions. Journal of Geophysical Research, 91(B5), 4673–4676.

Nye, J.F. (1985) Physical properties of crystals. Their representation by tensors and matrices. Oxford University Press, Oxford.

Pasternak, M.P., Nasu, S., Wada, K., and Endo, S. (1994) High-pressure phase of magnetite. Physical Review B, 50, 6446–6449.

Reichmann, H.J. and Jacobsen, S.D. (2004) High-pressure elasticity of a natural magnetite crystal. American Mineralogist, 89, 1061–1066.

Reichmann, H.J., Angel, R.A., Spetzler, H.A., and Bassett, W.A. (1998) Ultrasonic interferometry and X-ray measurements on MgO in a diamond anvil cell. American Mineralogist, 83, 1357–1360.

Sinogeikin, S.V. and Bass, J.D. (2001) Single-crystal elasticity of γ-$(Mg_{0.91}Fe_{0.09})_2SiO_4$ to high pressures and to high temperatures. Geophysical Research Letters, 28, 4335–4338.

Sinogeikin, S.V., Bass, J.D., Kavner, A., and Jeanloz, R. (1997) Elasticity of natural majorite and ringwoodite from the Catherwood meteorite. Geophysical Research Letters, 24, 3265–3268.

Sinogeikin, S.V., Bass, J.D., and Katsura, T. (2003) Single-crystal elasticity of ringwoodite to high pressures and high temperatures: implications for 520 km seismic discontinuity. Physics of the Earth and Planetary Interiors, 136, 41–66.

Spetzler, H.A., Chen, G., Whitehead, S., and Getting, I.C. (1993) A new ultrasonic interferomter for the determination of equation of state parameters of submiilimter single crystals. Pure and Applied Geophysics, 141, 341–377.

Wang, H. and Simmons, G. (1972) Elasticity of some mantle crystal structures 1. Pleonaste and hercynite spinel. Journal of Geophysical Research, 77, 4379–4392.

Weidner, D.J., Sawamoto, H., Sasaki, S., and Kumazawa, M. (1984) Single crystal elastic properties of the spinel phase Mg_2SiO_4. Journal of Geophysical Research, 89(B9), 7852–7860.

Yoneda, A. (1990) Pressure derivatives of elastic constants of single crystal MgO and $MgAl_2O_4$. Journal of Physics of the Earth, 38, 19–55.

Yutani, M., Yagi, T., Yusa, H., and Irifune, T. (1997) Compressibility of calcium ferrite-type $MgAl_2O_4$. Physics and Chemistry of Minerals, 24, 340–344.

MANUSCRIPT RECEIVED OCTOBER 18, 2005
MANUSCRIPT ACCEPTED MARCH 5, 2006
MANUSCRIPT HANDLED BY G. DIEGO GATTA